PHYSICAL REVIEW B **68**, 121401(R) (2003)

Geometry-based simulation of submonolayer film growth

Maozhi Li,[1] M. C. Bartelt,[2] and J. W. Evans[1]
[1]*Department of Mathematics and Ames Laboratory-USDOE, Iowa State University, Ames, Iowa 50011, USA*
[2]*Department of Chemistry and Materials Science, Lawrence Livermore National Laboratories, Livermore, California 94550, USA*
(Received 14 July 2003; published 17 September 2003)

A geometry-based simulation (GBS) strategy is developed for modeling film growth, which avoids explicit treatment of the terrace diffusion of adatoms and their aggregation with islands—a computationally expensive component of either atomistic simulation or continuum analysis. GBS characterizes island growth in terms of capture zones (CZ's), and implements simple but realistic geometric rules to incorporate crucial spatial aspects of the island nucleation process, i.e., nucleation nearby CZ boundaries. This approach reliably predicts island size distributions and spatial correlations, and is especially efficient for highly reversible island formation.

DOI: 10.1103/PhysRevB.68.121401 PACS number(s): 81.15.Aa, 05.70.Ln, 68.55.Ac, 81.10.Aj

Studies of the initial stage of film growth have attracted intense interest since the 1960s because of its importance to the development of subsequent film morphology and properties.[1] Initially, film growth involves competition between nucleation and growth of islands, mediated by diffusion of deposited atoms. Of key interest is detailed characterization of the island distribution, both sizes and spatial arrangement. This effort fits within a broader goal of first elucidating and then controlling the formation of various far-from-equilibrium nanostructures.

Traditional rate equation treatments of submonolayer deposition incorporate a mean-field (MF) description of adatom capture by islands. These MF treatments, which have their origin in classic Smoluchowski treatments of aggregation,[2] are quite successful in predicting the behavior of the mean island density or size,[1] but they fail to describe the island size distribution.[3–5] Precise results for the island distribution can be obtained in kinetic Monte Carlo (KMC) simulation studies of atomistic film growth models.[3] However, this approach often yields only limited insight into the essential physics, compared with analytic theories. Furthermore, KMC is computationally expensive for highly reversible island formation and for large characteristic lengths.

Thus, there is interest in developing alternative approaches, either beyond-MF rate equation theories[6–9] or efficient ''coarse-grained'' simulation algorithms[10–13] which reliably connect underlying atomistic processes to large-scale morphology. In either case, to correctly predict the island distribution, such formulations must account for the feature[5] (neglected in MF) that larger islands have on average significantly larger capture zones[5,13,14] (CZ's) for depositing atoms. This, in turn, requires a realistic treatment of the spatial aspects of the nucleation process,[9] which is readily achieved in coarse-grained simulation algorithms. These algorithms typically adopt a continuum description for the edge positions of islands, and determine their growth deterministically from solution for the adatom density of continuum diffusion equations with adsorbing boundary conditions at island edges.[10,13] Nucleation is still treated stochastically at a rate reflecting the local adatom density.[10] Correct treatment of island growth shapes is still challenging, but it might be addressed by an approach which combines an atomistic description of island edge evolution with continuum diffusion equations.[12]

In this Rapid Communication, however, we present different geometry-based simulation (GBS) strategy for modeling of film growth, which sidesteps any explicit treatment of terrace diffusion, a computationally expensive step either within an atomistic KMC simulation or a continuum diffusion equation formulation. This is achieved in GBS by utilizing a geometric formulation of island growth in terms of suitably constructed CZ's. In addition, we incorporate an explicit geometry-based prescription of spatial aspects of the island nucleation process, a feature which is crucial to correctly describe development of the island distribution. Specifically, we incorporate an initial ''transient'' regime of random nucleation outside of depletion zones, which expand around new islands. This regime is connected to a subsequent ''steady-state'' regime wherein islands are nucleated nearby the boundaries between CZ's. Comparison of results against KMC simulations confirms the capability of GBS to recover even subtle correlations in the island size and CZ distributions. Just as significantly GBS provides a versatile tool to explore and elucidate the effect of different prescriptions of nucleation on the development of the island distribution. It is particularly efficient for strongly reversible island formation. Finally, we note that GBS can also be applied in more complex growth scenarios.

We now describe the ''classic'' atomistic film growth models considered here: atoms are deposited randomly with flux F on a surface with a square lattice of adsorption sites; isolated adsorbed (ad)atoms hop to adjacent sites with rate h; in the simplest case (critical size $i=1$), adatoms irreversibly nucleate new islands upon meeting other adatoms, and irreversibly aggregate with existing islands upon reaching their edges. Islands restructure to maintain near-square shapes after each aggregation event. Atoms deposited on top are immediately incorporated at the island edge.[3] To explore the capability of our GBS approach to describe behavior for reversible island formation, we also consider models with critical size $i=2$ and 3 in which only clusters of more than i adatoms form stable islands.[1] To maximize reversibility for $i=2$ and 3, we allow singly bonded adatoms in substable clusters to detach by hopping with the same rate h as isolated adatoms. Below, coverage is denoted by $\theta=Ft$.

As indicated above, these models can be analyzed ''exactly'' by KMC simulation or approximately by MF rate

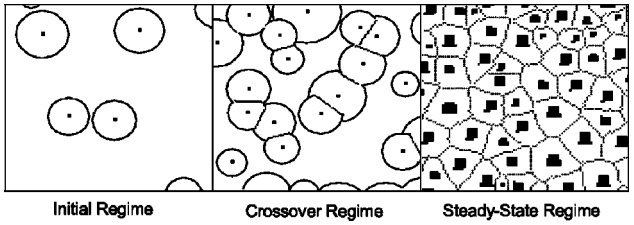

FIG. 1. Schematic of (a) initial, (b) crossover, and (c) steady-state regimes described in GBS algorithm. The figures show expansion and collision of DZ's, followed by formation of CZ's. Black squares denote islands; solid (dashed) lines denote DZ (CZ) boundaries.

equations. Here, instead we use GBS (and compare results with KMC). However, before describing the details of our GBS algorithm, it is useful to extract some insight from rate equation treatments which will be exploited in developing GBS algorithm. First, in these treatments, the local nucleation rate is taken as proportional to the product of local densities of adatoms and critical clusters, the latter scaling like the ith power of the adatom density (see Appendix). Second, rate equations for average adatom and island densities show that film growth occurs via an initial transient regime, where the adatom density builds up due to deposition, followed by crossover at $\theta^* \sim (h/F)^{-2/(i+3)}$ to a steady-state regime where gain of adatoms due to deposition is roughly balanced by loss due to aggregation with islands. Also, the mean island density at crossover is far below that in the steady-state regime (for large h/F), so most island nucleation (and also most island growth) occurs in the steady-state regime.[15]

We now describe our new GBS algorithm, which is tailored separately to each of three regimes shown schematically in Fig. 1. GBS simply involves implementing island nucleation (in all regimes) and growth [in regime (c)] according to the rules described below with the specified rates.

(a) In the initial regime, nucleated islands are surrounded by growing, but as yet nonoverlapping depletion zones (DZ's). Inside a DZ, the adatom density N_1 is significantly depleted from its ''background'' value of θ due to aggregation with the growing island. We define radius $R_{DZ}(t)$ of the growing DZ so that the integrated inhomogeneous nucleation rate near an island is recovered by assuming homogeneous nucleation outside the DZ at rate corresponding to uniform ''background'' $N_1 = \theta$.[16] A simple analytic form is constructed for $R_{DZ}(t) \sim (h\,\delta t)^{1/2}$ based on solution of the time-dependent diffusion equation for growth of an isolated island. Here, δt denotes the time since nucleation. Thus, in our growth algorithm, we nucleate at randomly chosen locations outside the DZ's at this uniform rate. Note that island growth is not significant in this regime and can thus be ignored (see above).

(b) In the crossover regime, DZ's start to overlap, since $R_{DZ} \sim (h\,\delta t)^{1/2}$ grows to roughly the mean island separation at θ^*. See Ref. 15. This initiates formation of so-called capture zones (CZ's) described under (c). Nucleation occurs randomly outside DZ's as above, and along developing CZ boundaries at a suitable rate (see Appendix). Often this regime can be ignored when neither island nucleation nor growth are significant.

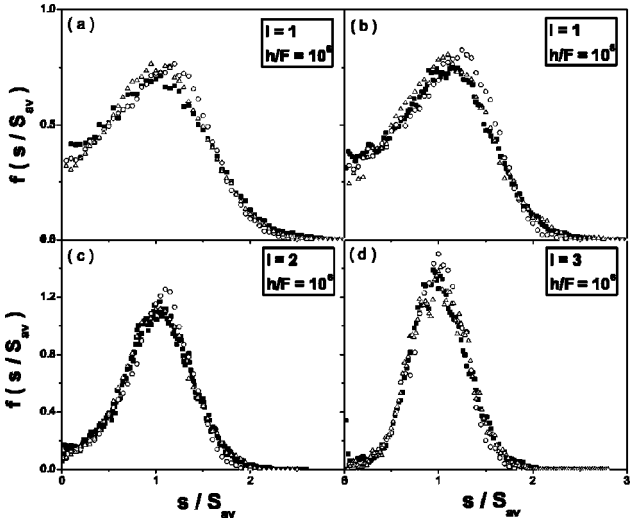

FIG. 2. Scaled island size distributions $f(s/S_{av})$ vs scaled size s/S_{av} for 0.1 ML: (a) $i=1$; (c) $i=2$; (d) $i=3$, for $h/F=10^6$; (b) $i=1$ with $h/F=10^8$. Basic (○) and refined (△) GBS, and KMC (■).

(c) In the final steady-state regime, the surface would be entirely covered by overlapped DZ's were these allowed to expand indefinitely. Instead as DZ's collide they are converted to CZ's, which in regime (c) tessellate the surface with one island per CZ. CZ's are ideally constructed from solution of the adatom diffusion equation for the steady state N_1 so that their areas are proportional to the total growth rate of the island contained within[13]—the sum of contributions due to diffusion mediated aggregation, as determined from N_1, and from deposition on top of islands. We reliably approximate the CZ's by ''edge cells'', whose boundaries are equidistant from the edges of nearby islands,[13,14] thus avoiding solution of the diffusion equation. In our basic GBS algorithm, we implement nucleation only along CZ boundaries, where N_1 and thus the nucleation rate is relatively large. The nucleation rate per unit length along CZ boundaries reflects the integrated nucleation rate orthogonal to CZ boundaries as determined from an approximation for the steady state N_1. See the Appendix. At least for small θ, this nucleation rate varies with the local distance L between the CZ boundary and the nearest island edge roughly like L^{2i+3}.

Unlike KMC, our GBS approach is readily amenable to exploring various prescriptions of nucleation. First, we show results from the basic GBS algorithm described above, then refine it to give better prediction of spatial correlations. We have also tested other instructive choices.[17]

Basic GBS Results. Figure 2 shows GBS results for the density of islands of s atoms, $N_s \approx (N_{isl}/S_{av}) f(s/S_{av})$ versus s (at 0.1 ML), for various i and h/F, and compares these directly with KMC results. Here N_{isl} (S_{av}) denotes the mean island density (size). GBS describes quite well the shape of the island size distribution with only a slight overestimate of peak height (which is corrected below). Importantly, GBS recovers scaling with increasing h/F [Fig. 2(a,b)]. GBS also produces the non-MF variation of the mean CZ area A_s for

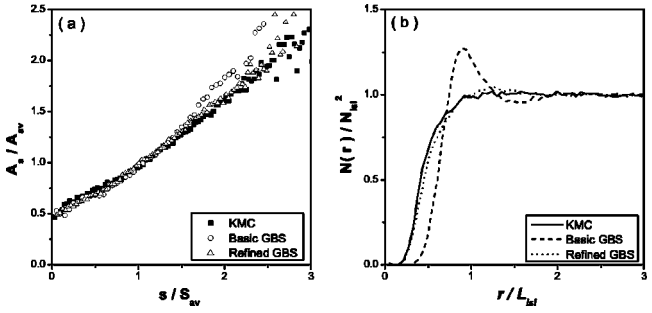

FIG. 3. (a) Size dependence of CZ areas; (b) island-island pair correlations for separation r, for $i=1$, $h/F=10^6$, at 0.1 ML. Comparison of basic, refined GBS, and KMC.

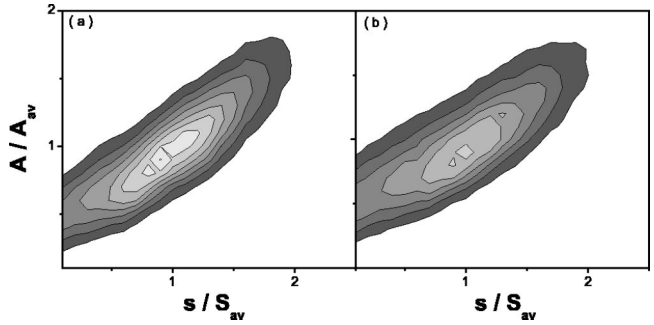

FIG. 4. Contour plots of the scaled JPD $F(s/S_{av},A/A_{av})$ vs scaled island size s/S_{av} and CZ area A/A_{av} for $i=1$, $h/F=10^6$, 0.1 ML: (a) refined GBS; (b) KMC.

islands of size s versus s [Fig. 3(a)].

The capability of our algorithm to predict island size distributions and scaling depends critically on a realistic treatment of nucleation. As emphasized by Ratsch *et al.*,[10] nucleation is stochastic, but not spatially random [except early in regime (a)]. Spatial aspects and persistence of nucleation in regime (c) are critical.[9] Most significant is the localization of nucleation nearby CZ boundaries in regime (c), where the steady state N_1 has higher values. Localization is enhanced for larger i since the nucleation rate scales like $(N_1)^{i+1}$. Additional support for this localized nucleation picture[18] comes from using KMC simulations to track positions of recently nucleated islands, and even from our analysis of low-energy electron microscopy data[19] for nucleation processes.

However, spatial correlations of island centers obtained from our basic GBS algorithm for $i=1$ reveal excessive depletion of the population of nearby islands compared to ''exact'' KMC. See Fig. 3(b). This is understood since nucleation positions are actually spread about CZ boundaries creating closer island pairs. However, we can make a simple refinement to our basic GBS algorithm (with negligible computational cost) to quite accurately recover these spatial correlations, and to even further improve the agreement of island size distributions with KMC.

Refined GBS results. In refined GBS, now each time we pick a nominal nucleation position (exactly) on a CZ boundary in regime (c), the new island is not nucleated exactly at that point, but rather located randomly within a neighborhood of radius gL centered on that point. (Here L is the distance to the nearest island edge, and $g<1$ avoids overlap of this region with islands.) To best reflect the actual spread of nucleation positions about CZ boundaries, we choose g so that the standard deviation for this uniform (but confined) nucleation distribution about the CZ boundary mimics that for the physical distribution $\propto(N_1)^{i+1}$. The standard deviation for the latter distribution is estimated using the analytic solution for the steady-state adatom density N_1 in a circular geometry (see the Appendix) in which the CZ radius (where $dN_1/dr=0$) exceeds the island radius (where $N_1=0$) by L. We find that $g\approx 0.7$ for $i=1$, with smaller values for $i>1$. Increasing g from zero (in the basic GBS algorithm) to this value significantly changes the island spatial correlations to match KMC, and also slightly modifies the island size distribution and the mean CZ area versus size to match KMC closely for $i=1$ and near perfectly for $i>1$. See Figs. 2 and Fig. 3.

Next, we consider the joint probability distribution (JPD), for the density per site $N_{s,A}\approx N_{isl}/(S_{av}A_{av})F(s/S_{av},A/A_{av})$ of islands with size s and CZ area A.[6,9] Here, $A_{av}=1/N_{isl}$ is the average CZ area. This JPD contains extensive information on the island distribution. Results in Fig. 4 for $i=1$ with $h/F=10^6$ at 0.1 ML show that refined GBS recovers the broad distribution of CZ areas for each island size, and the non-mean-field variation of mean capture zone area, $A_s=\Sigma_A A N_{s,A}/N_{isl}$ with s, as determined from KMC. We note that neglect of the spatial aspects of nucleation in analytic treatments as in Ref. 7 leads to unphysical (singular) JPD's in the scaling limit.[9]

Finally, we note that GBS is also versatile in allowing treatment of deposition models with other types of adatom dynamics, e.g., nucleation mediated by exchange of adatoms with the substrate,[20] or conventional nucleation with adatom desorption at rate $d>0$.[21] For the latter, we have checked that a GBS treatment correctly recovers the transition in the island size distribution from the form of Fig. 2 for small d to a monotonically decreasing form for larger d.

In summary, we have developed a GBS approach for submonolayer film growth, which elucidates and exploits key spatial aspects of the island nucleation process, and which correctly and efficiently recovers exact KMC results.

M.L. and J.W.E. were supported by NSF Grant Nos. EEC-0085604 and CHE-0078596 at Ames Laboratory-U.S. DOE operated by ISU under Contract No. W-7405-Eng-82. M.C.B. was supported by the U.S. DOE at UC Lawrence Livermore NL under contract No. W-7405-Eng-48.

APPENDIX: LOCAL NUCLEATION RATES

The local densities of critical clusters N_i and adatoms N_1 satisfy a quasiequilibrium Walton relation $N_i\approx c_i(N_1)^i$, where c_i reflects the number of cluster configurations.[1] (Note that the models considered here, detachment of singly bonded atoms is not inhibited). The local nucleation rate satisfies[1] $K_{nuc}=\sigma_i h N_1 N_i\approx\sigma_i c_i h(N_1)^{i+1}$, where σ_i is the ''capture number'' for critical clusters.

Initial regime (a). If $A_{nuc}=A_{tot}-\Sigma_j \pi R_{DZ}(j)^2$ is the total area outside the DZ's for a system of total area A_{tot}, then the total nucleation rate is $K_{nuc}(tot)=\sigma_i c_i h\,\theta^{i+1}A_{nuc}$.

Crossover regime (b). Here we supplement the rate used in regime (a) with an estimated contribution from nucleation along partially formed segments of CZ boundaries created by the collision of circular DZ's. For points on the boundary segments of distance L from the nearest island edge, the nucleation rate per unit length scales like L^{2i+3}. See the analysis below.

Steady-state regime (c). For each island and CZ, labeled by j, we extract an effective island radius $R_{isl}(j)$ and CZ radius $R_{CZ}(j)$ from their areas. We then estimate the total nucleation rate within that CZ, $K_{nuc}(j) \approx \sigma_i c_i h \int_{R_{isl}}^{R_{CZ}} 2\pi r [N_1(r)]^{i+1} dr$, where $N_1(r) \propto (F/h) \times [\frac{1}{2} R_{CZ}^2 \ln(r/R_{isl}) + \frac{1}{4}(R_{isl}^2 - r^2)]$ is the steady-state adatom density in an annular region $R_{isl} < r < R_{CZ}$, with vanishing density at $r = R_{isl}$, and vanishing flux at $r = R_{CZ}$ (dropping the label j). For $R_{isl}(j) \ll R_{CZ}(j)$, one has $K_{nuc}(j) \sim R_{CZ}(j)^{2i+4}$, ignoring log corrections. Thus, if all this nucleation is reassigned to the CZ perimeter, the nucleation rate per unit length scales like $R_{CZ}(j)^{2i+3}$. $K_{nuc}(tot) = \Sigma_j K_{nuc}(j)$ can be compared with the total island growth rate, $F \times$(system size), to determine the relative frequency of nucleation versus island growth events. If a nucleation event is selected, then a CZ boundary site is chosen with the appropriate weight.

[1] J.A. Venables, Philos. Mag. **27**, 697 (1973).
[2] M. von Smoluchowski, Phys. Z. **17**, 557 (1916).
[3] M.C. Bartelt and J.W. Evans, Phys. Rev. B **46**, 12 675 (1992); Surf. Sci. **298**, 421 (1993).
[4] G.S. Bales and D.C. Chrzan, Phys. Rev. B **50**, 6057 (1994).
[5] M.C. Bartelt and J.W. Evans, Phys. Rev. B **54**, R17 359 (1996).
[6] P.A. Mulheran and D.A. Robbie, Europhys. Lett. **49**, 617 (2000).
[7] J.G. Amar, Mihail N. Popescu, and Fereydoon Family, Phys. Rev. Lett. **86**, 3092 (2001).
[8] A. Zangwill, Nature (London) **411**, 651 (2001).
[9] J.W. Evans and M.C. Bartelt, Phys. Rev. B **66**, 235410 (2002).
[10] C. Ratsch, M.F. Gyure, S. Chen, M. Kang, and D.D. Vvedensky, Phys. Rev. B **61**, R10 598 (2000).
[11] C. Ratsch, M.F. Gyure, R.E. Caflisch, F. Gibou, M. Petersen, M. Kang, J. Garcia, and D.D. Vvedensky, Phys. Rev. B **65**, 195403 (2002).
[12] G. Russo, L.M. Sander, and P. Smereka (unpublished).
[13] M.C. Bartelt, A.K. Schmid, J.W. Evans, and R.Q. Hwang, Phys. Rev. Lett. **81**, 1901 (1998); M.C. Bartelt, C.R. Stoldt, C.J. Jenks, P.A. Thiel, and J.W. Evans, Phys. Rev. B. **59**, 3125 (1999).
[14] P.A. Blackman and P.A. Mulheran, Phys. Rev. B **53**, 10 261 (1996).
[15] Mean island density (N_{isl}), size ($S_{av} = \theta/N_{isl}$), and separation ($L_{isl} = N_{isl}^{-1/2}$) satisfy the following: $N_{isl}^* \sim (h/F)^{-\chi^*} \ll N_{isl}^{ss} \sim (h/F)^{-\chi}$, since $\chi^* = (i+1)/(i+3) > \chi = i/(i+2)$; $S_{av}^* \ll S_{av}^{ss}$; and $R_{DZ}^* \sim (h/F)^{1/2} (\theta^*)^{1/2} \sim L_{isl}^* = (N_{isl}^*)^{-1/2}$. Here $*[ss]$ denote values at $\theta = \theta^* [\theta = O(1)]$.
[16] Matching the exact rate of nucleation near a circular island (radius R_{isl}) to that for uniform nucleation outside a DZ (radius R_{DZ}) implies $\int_{r>R_{isl}}^{R^+} 2\pi r dr N_1(r,t)^{i+1} = \int_{r>R_{DZ}(t)}^{R^+} 2\pi r dr (\theta = Ft)^{i+1}$, where R^+ is a suitable upper cutoff.
[17] Nucleating at the position most distant from all island edges (for a large finite system) produces artificially ordered island array, similar to a previous study which solved the continuum diffusion equation and nucleated at the global maximum of N_1 (Ref. 10).
[18] J.W. Evans, J.B. Hannon, M.C. Bartelt, and G.L. Kellog, Bull. APS **45**, 363 (2000).
[19] J.B. Hannon M.C. Bartelt, N.C. Bartelt, and G.L. Kellogg, Phys. Rev. Lett. **81**, 4676 (1998).
[20] D.D. Chambliss and K.E. Johnson, Phys. Rev. B **50**, 5012 (1994).
[21] P. Jensen, H. Larralde, and A. Pimpinelli, Phys. Rev. B **55**, 2556 (1997).